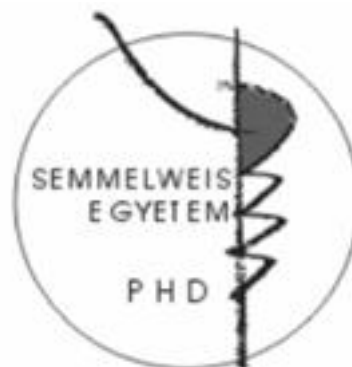# Exploring the nanomechanics of desmin

Theses of the doctoral dissertation

Balázs Kiss, M.D.

Semmelweis University
Doctoral School of Basic Medicine

Supervisor: Prof. Miklós Kellermayer, D.Sc.

Reviewers: Róbert Horváth, Ph.D, research professor,
           Zoltán Prohászka, D.Sc, research professor.

Chair of the examination board: Prof. Erzsébet Ligeti, member of the
                                      Hungarian Academy of Sciences
Members of the examination board: Prof. László Buday, D.Sc.
                                      Mihály Kovács, Ph.D, research professor.

Budapest
2012

Introduction

Desmin is the intermediate filament of smooth and striated muscle. Intermediate filaments (IF) appear to be 8-12-nm-thick apolar polymers on electron micrgoraphs and are important components of the cytoskeleton, a three-dimensional network in the cytoplasm of metazoan cells. The exact role of desmin filaments in muscle cells still remains unclear however; they presumably form a stable mechanical skeleton and might participate in signal transduction pathways. Desmin is characteristic and specific to the majority of muscle tissues except to the smooth muscle layer of some large elastic arteries and veins where vimentin forms the IF-network. In striated muscle it forms a complex around the Z-discs whereas in smooth muscle it associates with the "dense body" and anchors the contractile apparatus to the cell membrane. The 53 kDa molecule weight desmin displays a similar molecular architecture to other IF-s in which a central rod region, composed of four α-helical domains interrupted with three linker sequences, is flanked by head and tail domains. The periodic pattern of hydrophobic amino acids (leucine, isoleucine and valine) inside the α-helical domains plays a fundamental role in stabilizing the „coiled-coil" structure of desmin dimer. Seven amino acid residues form a so called heptad repeat in which the 1st and 4th residues (core positions) are generally occupied by hydrophobic amino acids and these are aligned on the same side of the α-helix.

IF-s polymerize spontaneously in low ionic strength medium (i.e. Na^+ or Mg^{2+} concentration below 0.01 M) without the requirement of ATP or GTP. The first step of the polymerization is the formation of a ~48 nm long coiled-coil formed by two parallel oriented desmin monomers and stabilized by the abovementioned apolar interactions. Further polymer structures are stabilized by an electrostatic interaction between neighboring chains: two staggered antiparallel dimers form a tetramer where ~15 nm is the length of the displacement. Tetramers associate laterally, composing the 10-mm-diamter 60-nm-long unit-length filaments (ULFs), followed by longitudinal annealing of ULFs into loosely-packed filaments of several μm-length, and finally by the radial compaction to their diameter (~10 nm). Inside the structure of mature filaments further assembly entities can be resolved with ultrastructural analysis: thicker protofibrils and thinner protofilaments.

Intermediate filaments play fundamental roles in tissue and cell mechanics, although the exact mechanisms of their mechanical function are still unclear. The mechanical role of intermediate filaments is particularly evident in diseases in which the loss of mechanical function and integrity of various tissues is associated with intermediate-filament-protein

mutations. In muscle contraction, the myofibrils have to withstand longitudinal strain but they need to be flexible against lateral forces. Increased stiffness upon mechanical stress can serve as a model to understand the desmin-related diseases, desminopathies. Mutations of desmin monomer usually manifest in muscular dystrophies and cardiomyopathies. The most frequent cause of these desminopathies is a single base substitution inside the α-helical domain of the desmin monomer which usually manifests in defective polymerization. Mutations involving conservative sequences in desmin head domain can result in distorted protein assembly in the early stages of polymerization; the distorted protein disassembles into its precursors which form aggregates that are deposited inside the cells. In muscle, where desmin integrates sarcomeric Z-discs, with other, neighboring Z-discs, with mitochondria, the cell nucleus and desmosomes, knock-out of the desmin gene results in sarcomeric ultrastructural changes and reduction of active and passive muscle forces. The stabilizing role of desmin in muscle cells is underlined by the observation that the severity of the structural damage is directly proportional to the loss of the desmin immunoreactivity (i. e. loss of desmin). Disappearance of desmin around the Z-discs alters the distribution of titin. Since titin presumably serves as a passive, longitudinal stabilizing element in muscle; it is feasible that an extrasarcomeric cytoskeleton (including desmin, α-actinin, plectin) stabilizes the intrasarcomeric cytoskeleton (titin, nebulin).

Research objectives

Because the hypothesized role of intermediate filaments are force transduction and mechanical stabilization of living cells my main objective was to characterize the elastic properties of desmin, the intermediate filament of muscle tissue. I planned to characterize the flexibility of purified surface-adsorbed single desmin filaments using atomic force microscopy (AFM)-based single-molecule force spectroscopy. Based on the knowledge of the elastic properties of desmin filaments and subunits my further aim was to propose and elaborate a model which supports the hypothesized role of desmin in force transduction. On these bases I constructed the following detailed experimental protocol:

1) Purification of desmin from chicken gizzard,
2) Specific detection of desmin using Western-blot,
3) Polymerization of desmin, time-dependence of polymerization,
4) AFM-based topographical analysis of mature desmin filaments,
5) Studying the elastic properties of desmin filaments,

6) *In situ* AFM on singe desmin filaments.

Besides the mechanical manipulation of single filaments I intended to define an elastic parameter based on the shape fluctuation analysis of surface-adsorbed desmin filaments which characterizes the whole filament width. This shape analysis could be performed using high-resolution surface scanning AFM. The resultant, second elastic parameter is independent from the previous one and could reliably characterize the total cross-section of desmin filaments in contrast to the first method in which one cannot exclude the possibility of manipulating subfilamentous structures with the tip of the AFM-cantilever.

My final objective was to study the elastic response of the building blocks of the desmin filament: protofilaments and protofibrils with the utilization of already assembled mature filaments. Keeping in mind that ionic interactions play an important role in stabilizing the filamentous structure I considered to decompose the mature filaments with divalent ion-specific chelators (ethylene glycol tetraacetic acid: EGTA and ethylene diamine tetraacetic acid: EDTA).

Materials and methods

Desmin was purified from chicken gizzard under denaturing conditions using anion-exchange chromatography, following tissue extraction with KI. Samples from the desmin-rich fractions were stored in 6 M urea on ice. Purity was estimated with densitometry on SDS-polyacrylamide gel electrophoretograms, and the presence of desmin was detected by Western-blot with specific anti-desmin antibody. The polymerization of desmin was initiated by the addition of either NaCl or $MgCl_2$ subsequent to the removal of urea with dialysis.

The elastic response of single molecules at a given force was measured using AFM. AFM is a high-resolution scanning probe device in which the deflection of a sharp cantilever tip is detected and magnified by a reflected laser beam which changes during the interaction between the tip and an elastic molecule. For mechanical manipulation surface-adsorbed desmin filaments under aqueous buffer conditions were stretched by moving the cantilever away from the surface. The force emerged in the molecule is calculated from the cantilever deflection whereas the extension is derived from the cantilever travel. The elastic behavior of single molecules can be studied from the registered force *versus* extension curves. The nonlinear elastic curves were fitted with the Wormlike Chain (WLC) entropic polymer model

which regards the molecule as an isotropic rod that is continuously flexible. The equation of this model represents the relationship between the following elastic parameters of a flexible chain: contour length which is the length measured along the contour of a molecule; the end-to-end length which corresponds to the extension during the stretch-release experiments and finally, the persistence length which is the measure of bending rigidity. Persistence length is the maximum length of the uninterrupted polymer chain persisting in a particular direction.
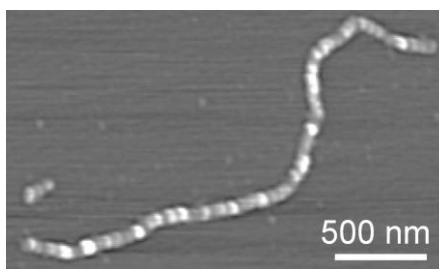
The persistence length of desmin can be assessed by analyzing the relationship between the end-to-end distance and contour length of surface-equilibrated filaments if we assume that the filaments had enough time to be equilibrated and their orientation and shape fluctuations on the surface is a two-dimensional projection of their unperturbed orientation in the aqueous buffer solution.

Structural unraveling of mature desmin filaments was carried out by the addition of Na-phosphate. To disrupt desmin filaments, samples were exposed to high concentrations of divalent cation chelators; Ca^{2+}-specific EGTA or Mg^{2+}-specific EDTA. Typical incubation times ranged between 2 hours for EDTA and 21 days for EGTA.

High-resolution images were recorded from negatively stained desmin filament samples and disassembly intermediates using transmission electron microscopy.

Results

Typical purification procedures yielded desmin of high, 97 % purity based on gel-electrophoretograms, protein concentration was assessed using Bradford-assay resulting in 1.37 mg/mL. Desmin polymerization was monitored through measuring absorbance due to light scatter at the wavelength of 320 nm as a function of time and proceeded at room temperature with a rate constant of $1.23 \cdot 10^{-3}$ s^{-1}. After two hours of incubation desmin assembly was more or less complete according to light scatter measurements. I found no systematic differences in the morphologies of desmin polymerized by the addition of either Na^+ or Mg^{2+}. Considering the 10 nm diameter of desmin filaments on electron micrographs the calculated real width of surface-adsorbed mature desmin filaments is ~50 nm which refers to a significant flattening (**Figure 1**). This flattening probably occurred as a result of the

Figure 1: Desmin filament on mica surface.

500 nm

different sample preparations (surface adsorption, dehydration) or of the sample commensurable radius of the AFM cantilever tip.

For mechanical manipulation desmin filaments, adsorbed to mica were captured with the tip of a flexible AFM cantilever. The filaments were then stretched by moving the cantilever away from the surface. The mechanically manipulated desmin displayed complex force responses. I identified four fundamental types of mechanical behavior: 1) initial
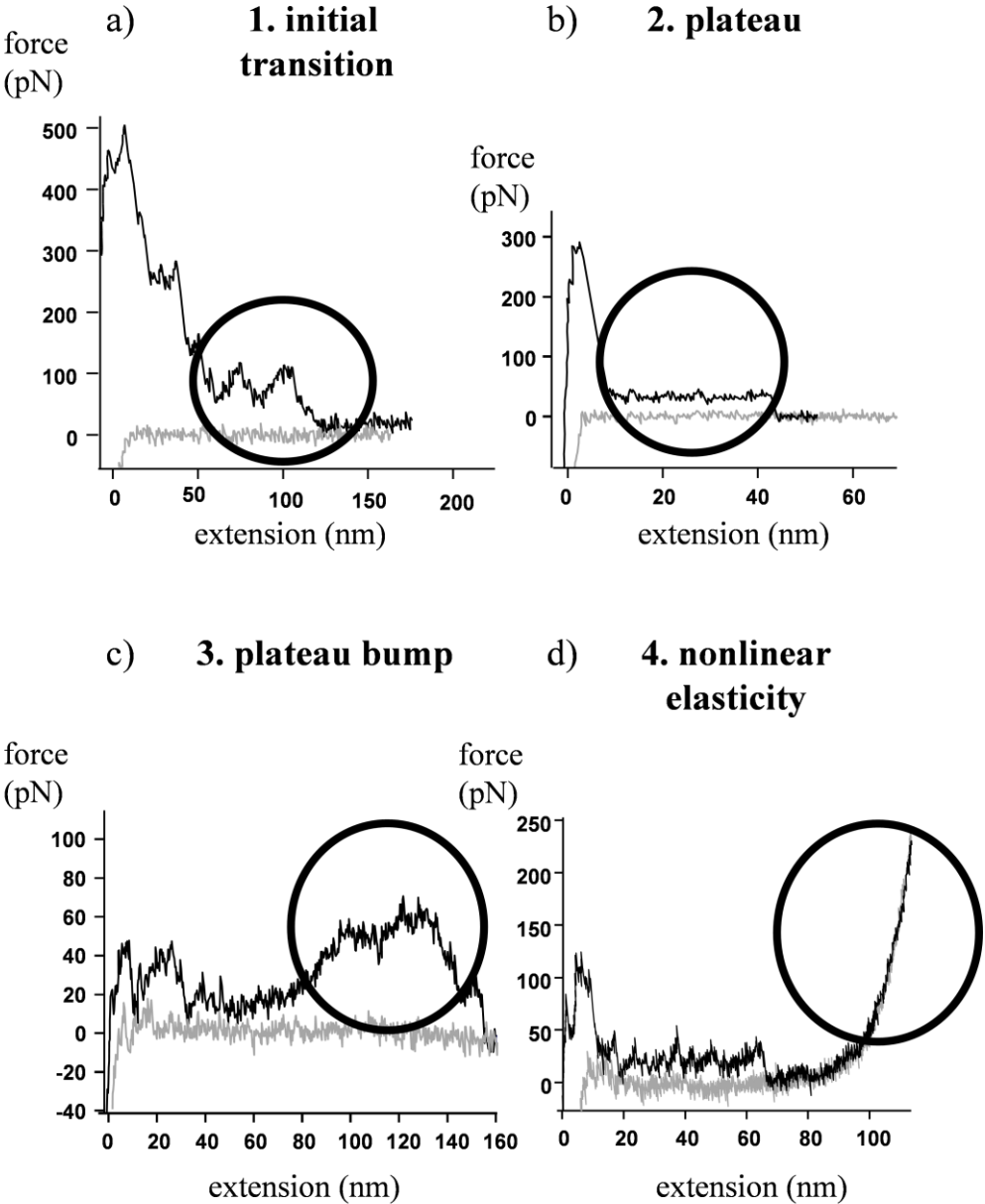
Figure 2: Characteristic force *vs.* extension curves of desmin. Every curve represents a complete stretch-release cycle. Black force traces refer to the stretch phase whereas the grey ones display the release.

transition, 2) force plateau 3) plateau bumps and 4) non-linear elasticity (**Figure 2**).

Initial transition is a force bump defined as a transient plateau with gradually ascending and descending limbs if the total length of the force response was less than 60 nm. Initial-bump spacing, force, total length of the transition and the number of bumps within the transition were analyzed and plotted as histograms. The initial-bump spacing histogram showed a multimodal distribution with peaks distributed at approximately 11, 22 and 33 nm. Similarly, the initial-bump force histogram also showed a multimodal distribution with peaks at approximately 20, 40 and 60 pN. The number of bumps per initial transition trace was most frequently two in the case of desmin filaments and did not exceed 4 bumps per transition.

The second characteristic feature in the elastic behavior of desmin is the so called force plateau. The force plateau is characterized by a more or less flat force trace during stretch that is usually parallel with the force retrace measured during relaxation and ends with a step-like decrease in force. I plotted plateau height (force) and plateau length histograms and I found no correlation between the plateau forces and lengths indicating that these parameters are independently determined during mechanical manipulation. The plateau height histogram suggested multimodal distribution with local maxima at 13, 26, 39 and 52 pN. Histogram peaks of the similarly multimodal distribution of plateau length are seen at ~12, ~24 and ~36 and 48 nm.

In the case of desmin tethers the length of which exceeded 60 nm (the length of ULF) the force bumps visible in the force traces were called plateau bumps. The plateau-bump force and plateau height histograms showed broad distributions with maxima centered around 25, 50, 75 pN; and 8, 16, 24 nm, respectively.

Long series of repetitive sawtooth force transitions were observed infrequently in stretch experiments where extension exceeded 200 nm. Often, sawtooth transitions were superimposed onto force plateaus. A transition is called a force sawtooth if it resembles a peak approached by non-linear increase in force and is followed by a sudden force drop devoid of intermediates and typically appears when a polymer chain displaying sudden, stepwise contour length increments is being stretched. The histogram of sawtooth transition forces, defined as the force at the peak of the sawtooth, suggests a multimodal distribution with peaks at integer multiples of ~30 pN. Forces up to several hundred pN were observed in the case of nonlinear elasticity.

The non-linear curves were fitted with the wormlike chain model of entropic elasticity to obtain the persistence length (measure of bending rigidity) of the mechanically manipulated

chains. The mean persistence length acquired from force measurement experiments was ~0.4 nm. This very low value might characterize the flexibility of a fully unfolded protein.
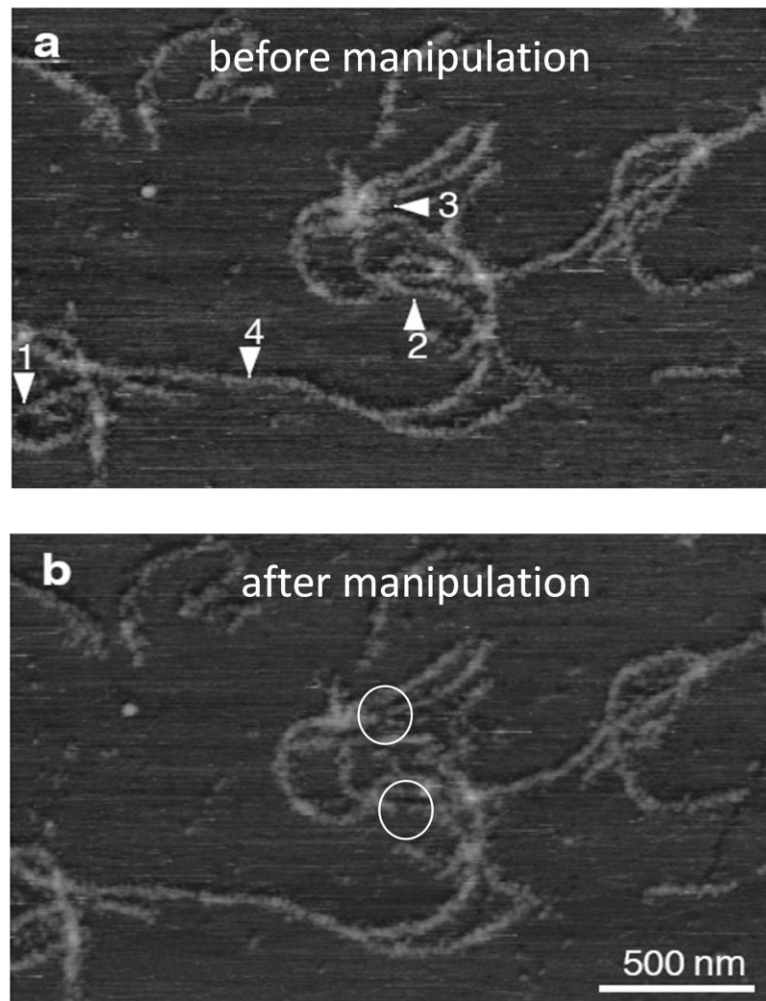

Figure 3: *In situ* AFM on desmin filaments. Arrowheads indicate the manipulation sites.

On specific sites of a topographic AFM image we could perform *in situ* force spectroscopy on single desmin filaments by moving the cantilever tip vertically. Mechanical manipulation of the filaments did not result in significant changes in the morphological appearance of the filaments; only in few cases a certain degree of material loss was observed (white circles in **Figure 3**) whereas complex, elastic force responses were registered in each indicated sites. This might indicate that entire filaments were not removed from the surface as a result of mechanical manipulation.

Phosphate treatment has been shown previously to induce the unraveling of keratin filaments on electron micrographs. The most prominent changes observed in phosphate-treated filaments were the decrease 1) in plateau bump spacing, 2) force plateau length, 3) sawtooth transition force and length gain, and the partitioning of the initial unbinding event into multiple (usually 3-4) short transitions.

Persistence length of filaments could be obtained by analyzing their global shape in terms of contour length and end-to-end distance which properly describes the bending rigidity of the 10-nm-wide mature desmin filaments. Plotting the mean square end-to-end distance *versus* contour length of surface-adsorbed filaments resulted in persistence lengths of ~0.45 µm which corresponds well with the persistence length of other intermediate filaments measured under equilibrium conditions. Modeling the desmin filament as a homogeneous rod one can estimate its elastic modulus which was found to be 3.7 MPa in case of desmin.

Upon treating the desmin filament sample with either EDTA or EGTA, thin fibrillar structures appeared beside mature filaments (**Figure 4**). Mature filaments were embedded in a meshwork of these thin fibrils. The height of mature filaments is relatively broadly distributed
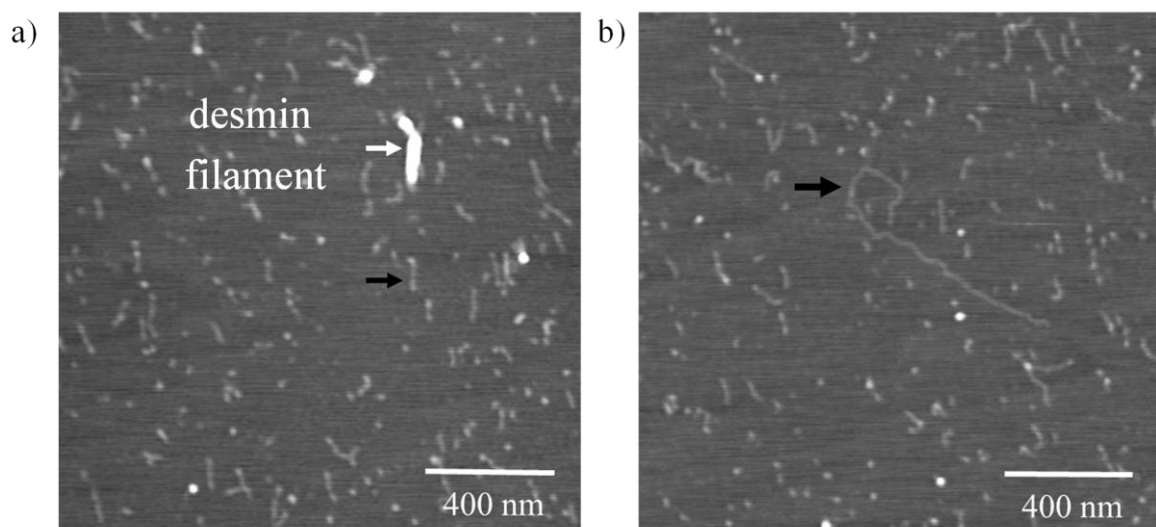

Figure 4: EGTA-treatment of desmin filaments (9 days incubation). Black arrows indicate the thin, fibrillar structures, white arrow points on a short desmin filament.

around a mean of 2.3 nm based on AFM images, whereas the histogram of mean thin fibril height displays a gaussian distribution with a mean of only 0.30 nm. The calculated real width of mature desmin filaments is 50.6 nm, and that of thin fibrils 25.5 nm, which indicates a significant flattening. Assuming a similar increase in cross-sectional dimensions for both the filament and the fibril; the true diameter of the thin fibrils is approximately 4.83 nm for circular cross-section and cylindrical shape. This value is in a good agreement with the diameter of keratin protofibrils determined by electron microscopy; therefore I postulate that mature desmin filaments fray into desmin protofibrils in the presence of EGTA or EDTA. The persistence length of desmin protofibrils is 0.05 µm based on the average shape fluctuations of surface-equilibrated proteins. The persistence length value calculated here compares well with the length of the desmin dimer; the estimated elastic modulus was 10.6 MPa on average, a factor of three greater than that of the mature filament.

The analysis of mature desmin filaments resulted in an average diameter of 10.3 nm based on electron micrographs, which is comparable with the electron microscopic reference diameter of mature filaments used to determine the increment factor for AFM analysis. Thin fibrils had an average diameter of 4.1 nm which is in accordance with the previous estimates of keratin protofibrils and proving the presence of stable, individual desmin protofibrils.

Conclusions

We propose the following empirical model which presents a possible scenario that may
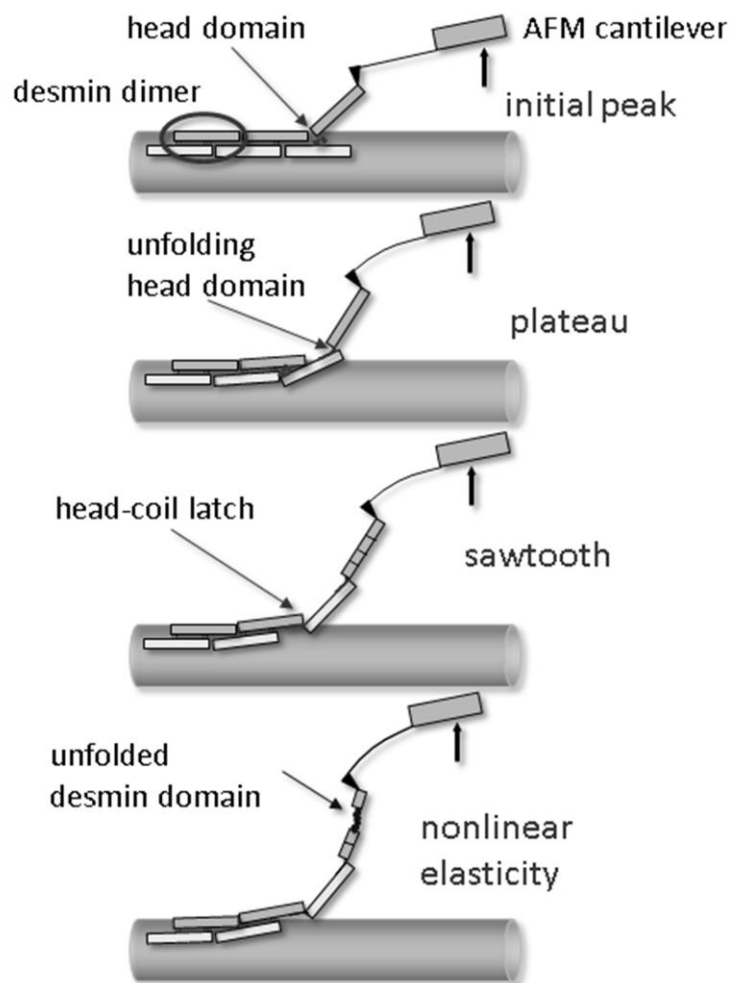
Figure 5: Schematic model of the hypothesized events associated with the nanomechanical manipulation of desmin filaments.

explain our observations (**Figure 5**). The main structural element which determines the flexibility of the desmin is the coiled-coil dimer. The weak lateral interaction between neighboring dimers may explain the **initial unbinding** event. This usually occurs in a two-step reaction, and is quite frequently reversible. There are more plausible mechanisms that

might explain the appearance of the **force plateau**: unzipping of protofilaments from the filament surface, unfolding of coiled-coil domains or sliding of coiled-coil desmin dimers past each other. If an elastic linkage, possibly via a head domain, is maintained between the lifted desmin dimer and its neighboring dimer left behind in the filament, and then further lifting of the cantilever results in continued mechanical perturbation. The elastic linkage may first become unfolded and stretched resulting in the dimers sliding past each other. The balance between sliding and further protofilament unzipping is probably determined by the balance of vertical (unzipping) force and the force acting in the axis of the tether (sliding force). Further stretch may result in slippage between unfolded dimers, causing **sawtooth** force transitions. If a new and stable binding occurs between neighboring dimers it might result in a repetitive sawtooth pattern on the force curve. **Nonlinear elasticity** can be the result of the further stretch of already unfolded desmin domains. Importantly, the unfolded desmin dimers need to be latched together laterally with sufficiently strong interactions to resist the high stretching forces. The **phosphate treatment** presumably weakens the lateral electrostatic interactions between desmin dimers.

Divalent cation chelators EGTA or EDTA interfered with the ionic interactions holding the desmin dimers laterally together (either due to their own charged nature or due to the withdrawal of Mg^{2+}). This interference resulted in the fraying and disassembly of mature
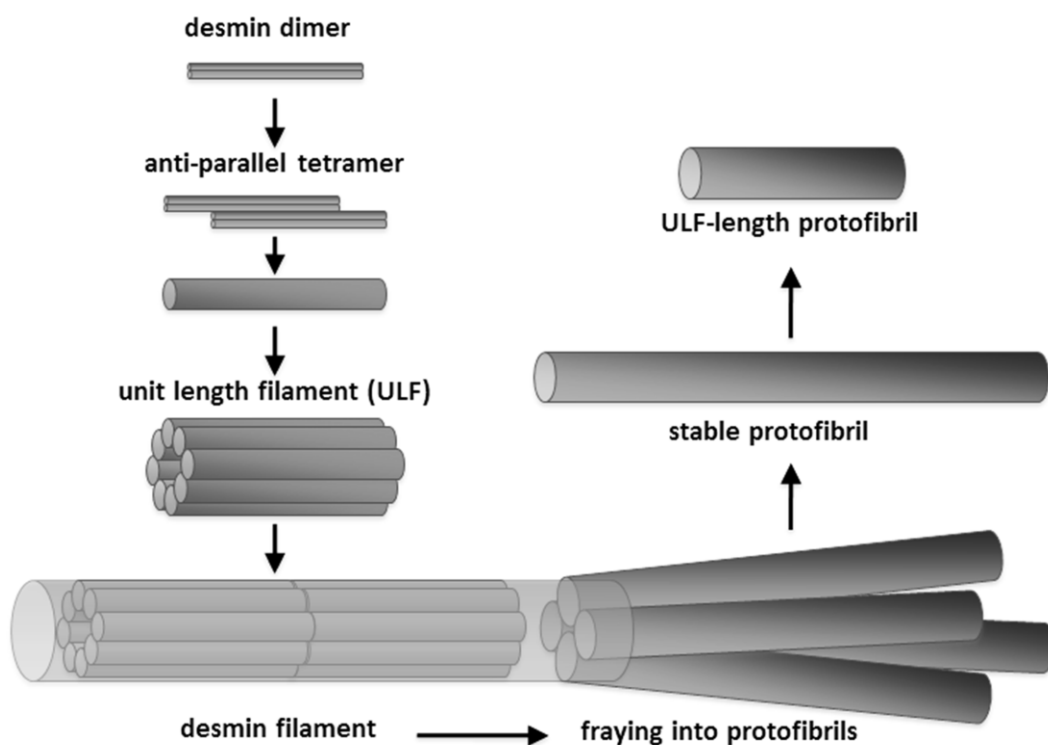
Figure 6: Desmin filament assembly and disassembly pathway.

filaments into 4-5 distinct, stable fibrillar structures identified as protofibrils (**Figure 6**). The appearance of distinct protofibrils suggests that the disassembly pathway of desmin may be quite different from its assembly pathway. During polymerization a full-filament-width (10 nm) ULF is being formed from tetramers and the longitudinal association of ULFs results in the assembly of desmin filament. Within the mature filament the interactions stabilizing the protofibril axially are stronger than the ones interconnecting them laterally, making the stable existence of protofibrils *in vitro* possible. Desmin filaments are not simply an enlarged version of the protofibril carrying the protofibril's material properties, not a homogeneous and isotropic structure. The desmin filament is therefore more flexible than expected based on the elastic properties of the underlying protofibril thus providing the muscle cells with large longitudinal tensile strength at large bending flexibility.

New scientific findings

Based on the above mentioned instrumentation I successfully identified the characteristic force responses of desmin purified from chicken gizzard as follows:

1) The initial transition trace was the most frequently observed force pattern characterized by two discrete 20-60 pN force steps. This may correspond to unbinding and removal of 45 nm long individual coiled-coil desmin dimers from the filament surface.

2) Force plateaus are characterized by constant force as a function of extension and resemble polymer desorption processes by protofilaments longer than 60 nm. Plateau bumps were superimposed on force plateaus in 16-nm steps. Conceivably, these force transitions appear as a result of unzipping or peeling protofilaments away from the surface of the desmin filament.

3) Non-linear force curves were observed upon further stretch. Considering that the persistence length was similar to that of unfolded protein molecules, it is conceivable that the non-linear force curves reflect the behavior of unfolded desmin monomers / protofilaments.

I measured the persistence length of desmin chains during the mechanical perturbation. The low, 0.4 nm average value most probably reflects the bending rigidity of fully unfolded desmin.

Based on the shape fluctuation analysis of surface-adsorbed desmin filaments I assessed the persistence length of the desmin filament using AFM imaging resulting in a value of 0.45 µm.

Upon the addition of divalent cation chelators EGTA or EDTA I disassembled the filaments on a time scale of hours to days into stable, thin fibrillar components. Based on topological considerations (circumference and diameter) the filamentous structures were identified as desmin protofibrils.

I addressed that the phosphate treatment presumably weakens the lateral electrostatic interactions between desmin dimers.

List of author's publications

1. **Kiss, B**, Karsai, A, Kellermayer, MS. (2006) Nanomechanical properties of desmin intermediate filaments. J Struct Biol 155: 327-339.

2. **Kiss, B**, Rohlich, P, Kellermayer, MS. (2011) Structure and elasticity of desmin protofibrils explored with scanning force microscopy. J Mol Recognit 24: 1095-1104.

3. Meyer, GA, **Kiss, B**, Ward, SR, Morgan, DL, Kellermayer, MS, Lieber, RL. (2010) Theoretical predictions of the effects of force transmission by desmin on intersarcomere dynamics. Biophys J 98: 258-266.